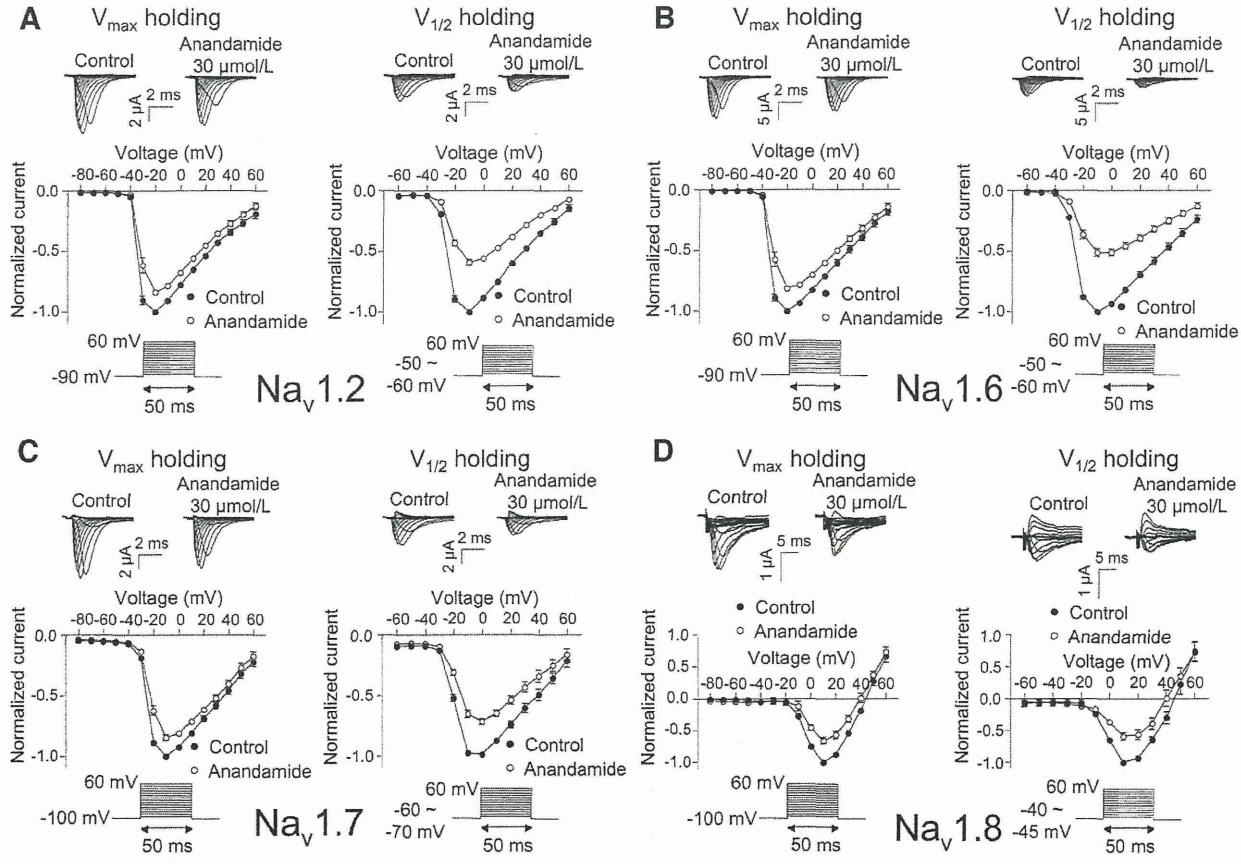

Figure 4. Effects of anandamide on I-V curves of sodium currents in oocytes expressing $Na_v1.2$ (A), $Na_v1.6$ (B), $Na_v1.7$ (C), and $Na_v1.8$ (D) α subunits with β_1 subunits. Currents were elicited by using 50-millisecond depolarizing steps between –80 and 60 mV in 10 mV increments from a V_{max} holding potential (left panel) and elicited by using 50-millisecond depolarizing steps between –60 and 60 mV in 10 mV increments from a $V_{1/2}$ holding potential (right panel); anandamide (30 μmol/L) was applied for 5 minutes; upper panel, representative I_{Na} traces from oocytes expressing $Na_v1.2$, $Na_v1.6$, $Na_v1.7$, and $Na_v1.8$ with β_1 subunits in both the absence and presence of 30 μmol/L anandamide; lower panel, effects of anandamide on representative I-V curves elicited from V_{max} holding potential (left panel) and $V_{1/2}$ holding potential (right panel) (closed circles, control; open circles, anandamide). Peak currents were normalized to the maximal currents observed from –20 to +10 mV. Data are represented as the mean ± SEM (n = 5–8).

activation and exhibit use-dependent block.[35–39] Our results show that anandamide shows a negative shift in the voltage dependence of inactivation and use-dependent block except for $Na_v1.8$ that are seen with other sodium channel blockers yet also shifts the steady-state activation in a depolarizing direction, suggesting that it may have different binding sites or allosteric conformational mechanisms for these sodium channel antagonists. Moreover, a resting-channel block, not an open-channel block, for $Na_v1.8$ may be a key for exploring the mechanism of sodium channel inhibition by anandamide in detail.

Several groups have evaluated antinociception by exogenous anandamide via CB_1 receptors.[8–10] Indeed, a recent review has shown that activation of both CB_1 and CB_2 receptors reduces nociceptive processing in acute and chronic animal models of pain.[40] Alternatively, other investigators have suggested that anandamide produces antinociception through a CB_1-independent mechanism. For example, anandamide antinociception is not blocked by pretreatment with the selective CB_1 antagonist SR141716A.[41] Rapid metabolism of anandamide to arachidonic acid has been shown to be one of the reasons for the failure of SR141716A to antagonize the effects of anandamide; in experiments, the ability of SR141716A to reverse anandamide antinociception was improved (but not completely) when anandamide metabolism to arachidonic acid was inhibited with coadministration of an amidase inhibitor, phenylmethylsulfonyl fluoride.[42] That study also demonstrated that cyclooxygenase did not alter the effects of anandamide, whereas it blocked the effects of arachidonic acid, suggesting a pain-inhibitory effect of anandamide by noncannabinoid mechanisms. Another recent study suggested that anandamide induced antinociception by stimulating endogenous norepinephrine release that activated peripheral adrenoceptors inducing antinociception, although whether the effect was caused through cannabinoid receptors remains unknown.[43]

This study indicates that sodium channel inhibition by anandamide is independent of signaling through cannabinoid receptors, because in recombinant experiments such as our present examination, the effects on channels or receptors can be excluded except for that expressed in membranes. Previous reports also indicate a direct effect of anandamide on sodium channels by demonstrating that sodium channel-related activities by anandamide in the brain may be independent of

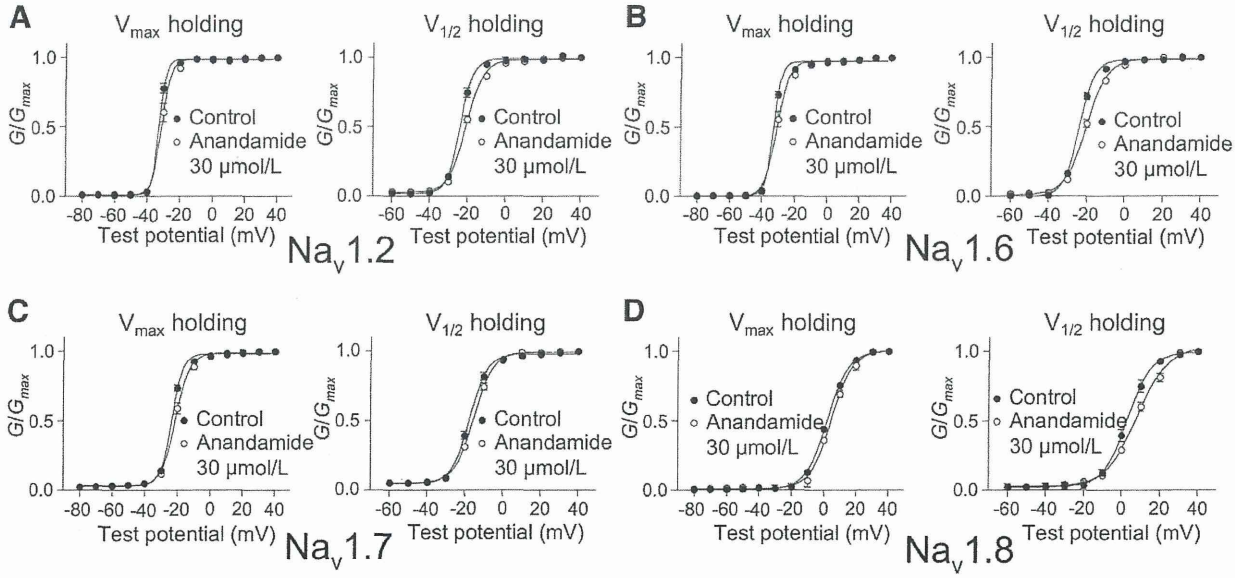

Figure 5. Effects of anandamide on channel activation in oocytes expressing $Na_v1.2$ (A), $Na_v1.6$ (B), $Na_v1.7$ (C), and $Na_v1.8$ (D) α subunits with β_1 subunits from V_{max} holding potential (left panels) or $V_{1/2}$ holding potential (right panels). Closed circles represent control; open circles indicate the effect of anandamide. Data are expressed as the mean ± SEM (n = 5–8). Activation curves were fitted to the Boltzmann equation; $V_{1/2}$ is shown in Table 1.

Table 1. Effects of Anandamide on Activation and Inactivation in Oocytes Expressing $Na_v1.2$, $Na_v1.6$, $Na_v1.7$, and $Na_v1.8$ α Subunits with β_1 Subunits

	$V_{1/2}$ (mV)					
	Holding V_{max}			Holding $V_{1/2}$		
	Control	Anandamide	Shift	Control	Anandamide	Shift
Activation						
$Na_v1.2$	−32.7 ± 0.3	−30.8 ± 0.7*	+1.9	−23.6 ± 0.6	−20.4 ± 0.6**	+3.2
$Na_v1.6$	−32.6 ± 0.3	−30.5 ± 0.7*	+2.1	−23.8 ± 0.5	−20.0 ± 0.6**	+3.8
$Na_v1.7$	−23.4 ± 0.4	−21.0 ± 0.8*	+2.4	−17.3 ± 0.7	−15.0 ± 0.7*	+2.3
$Na_v1.8$	2.2 ± 0.2	4.8 ± 0.8*	+2.6	3.3 ± 1.0	8.4 ± 1.1*	+3.3
Inactivation						
$Na_v1.2$	−51.4 ± 0.7	−56.6 ± 0.8**	−5.2			
$Na_v1.6$	−53.5 ± 0.8	−58.5 ± 1.0**	−5.0			
$Na_v1.7$	−64.3 ± 0.7	−68.4 ± 0.6**	−4.1			
$Na_v1.8$	−50.7 ± 1.4	−57.0 ± 1.9*	−6.3			

*P < 0.05.
**P < 0.01, compared with control (paired t test) (mean ± SEM; n = 5–7).

the presence of AM 251 (a CB_1 antagonist),[31] AM 251, AM 630 (a CB_2 antagonist) and capsazepine (a vanilloid receptor type 1 antagonist) do not interfere with anandamide suppression of sodium currents in DRG.[32] Therefore, we believe that the effects of anandamide on $Na_v1.2$, $Na_v1.6$, $Na_v1.7$, and $Na_v1.8$ α subunits are direct. Taken together, to the best of our knowledge, this is the first direct evidence to demonstrate the inhibitory effects and its mechanisms on neuronal sodium channel α subunits in recombinant experiment systems.

Several sodium channel α subunits are believed to be involved in the pathogenesis of inflammatory and neuropathic pain. Mutations in $Na_v1.7$ have been linked to inherited pain syndromes, including inherited erythromelalgia, that is characterized by episodes of burning pain, erythema, mild swelling in the hands and feet,[44] and paroxysmal extreme pain disorder (PEPD), which is characterized by severe rectal, ocular, and mandibular pain.[45] Recently, anandamide has been reported to inhibit resurgent current of wild-type $Na_v1.7$ and the PEPD mutants expressed in transfected human embryonic kidney 293 cells, and this inhibition was suggested as a therapeutic target for PEPD patients.[46] $Na_v1.8$ has demonstrated its ability to carry most current underlying the upstroke of the action potential in nociceptive neurons,[47] and the use of $Na_v1.8$ knockdown rats after antisense oligodeoxynucleotide treatment has demonstrated a role for $Na_v1.8$ in inflammatory pain,[48] whereas $Na_v1.8$ expression has been reported to increase in nerves proximal to injury sites in patients with chronic neuropathic pain.[49] In an infraorbital nerve injury model of rats, the level of $Na_v1.6$ protein was significantly increased proximal to the lesion site, suggesting a role of $Na_v1.6$ in neuropathic pain conditions.[50] However, these α subunits highly expressed in normal DRG have been reported to show diverse expression in DRG of inflammatory and neuropathic pain models. $Na_v1.7$ mRNA and protein increased in DRG after peripheral inflammation induced by

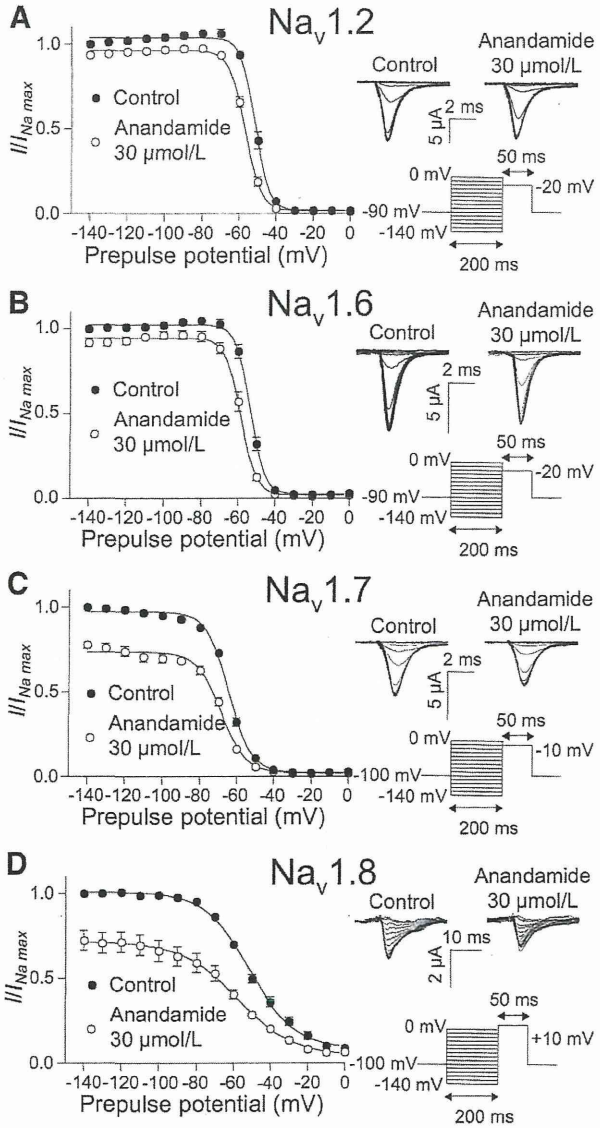

Figure 6. Effects of anandamide on inactivation curves in oocytes expressing $Na_v1.2$ (A), $Na_v1.6$ (B), $Na_v1.7$ (C), and $Na_v1.8$ (D) α subunits with β_1 subunits. Currents were elicited by a 50-millisecond test pulse to –20 mV for $Na_v1.2$ and $Na_v1.6$ or –10 mV for $Na_v1.7$ or +10 mV for $Na_v1.8$ after 200-millisecond (500-millisecond for only $Na_v1.8$) prepulses ranging from –140 mV to 0 mV in 10 mV increments from a holding potential of V_{max}; anandamide (30 μmol/L) was applied for 5 minutes; right panel, representative I_{Na} traces in both the absence and presence of anandamide; left panel, effects of anandamide on inactivation curves (closed circles, control; open circles, anandamide). Steady-state inactivation curves were fitted to the Boltzmann equation, and the $V_{1/2}$ values are shown in Table 1. Data are expressed as the mean ± SEM (n = 6–8).

carrageenan,[51,52] whereas $Na_v1.7$ protein decreased in the injured DRG after spared nerve injury in animals.[53] $Na_v1.8$ mRNA and protein increased in DRG neurons of rodents after injection of carrageenan into a hindpaw,[51,54,55] and yet peripheral nerve injury down-regulates $Na_v1.8$ mRNA and protein expression in the injured DRG.[29,53,56] Based on this evidence, suppression of sensory neuron sodium channel function by anandamide may be an important mechanism independent of the cannabinoid receptor. Because of the limitations of our experiments, further investigation is warranted to extrapolate our findings into clinical practice.

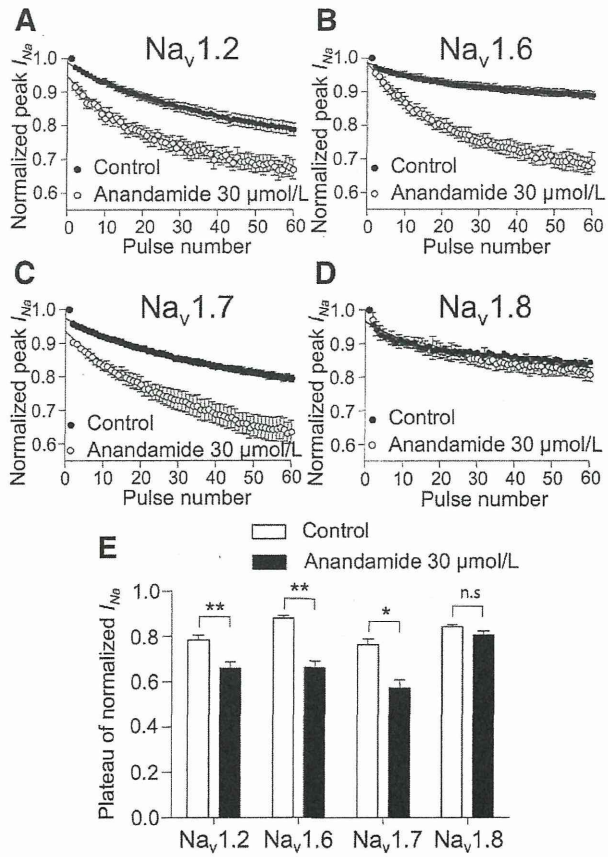

Figure 7. Use-dependent block of sodium channel on $Na_v1.2$, $Na_v1.6$, $Na_v1.7$, and $Na_v1.8$ α subunits with β_1 subunits of anandamide. Currents were elicited at 10 Hz by a 20-millisecond depolarizing pulse of –20 mV for $Na_v1.2$ and $Na_v1.6$, or –10 mV for $Na_v1.7$, or +10 mV for $Na_v1.8$ from a $V_{1/2}$ holding potential in both the absence and presence of 30 μmol/L anandamide; anandamide was applied for 5 minutes. Peak currents were measured and normalized to the first pulse and plotted against the pulse number (A, $Na_v1.2$; B, $Na_v1.6$; C, $Na_v1.7$; D, $Na_v1.8$). Closed circles represent control; open circles indicate the effect of anandamide. Data were fitted to the monoexponential equation, and values for fractional block of the plateau of normalized I_{Na} are shown in (E). Data are expressed as the mean ± SEM (n = 5–6). *P < 0.05 and **P < 0.01, compared with the control (paired t test).

In conclusion, anandamide at pharmacologically relevant concentrations inhibited sodium currents of $Na_v1.2$, $Na_v1.6$, $Na_v1.7$, and $Na_v1.8$ α subunits expressed in the *Xenopus* oocytes with differences in the effects on sodium channel gating. These results provide a better understanding of the mechanisms underlying the analgesic effects of anandamide, but further studies are needed to clarify the relevance of sodium channel inhibition by anandamide to analgesia.

DISCLOSURES

Name: Dan Okura, MD.

Contribution: This author helped data collection, data analysis, and manuscript preparation.

Attestation: Dan Okura approved the final manuscript and attests to the integrity of the original data and the analysis reported in this manuscript.

Name: Takafumi Horishita, MD, PhD.
Contribution: This author helped study design, data collection, data analysis, and manuscript preparation.
Attestation: Takafumi Horishita approved the final manuscript and attests to the integrity of the original data and the analysis reported in this manuscript, and also is the archival author.
Name: Susumu Ueno, MD, PhD.
Contribution: This author helped conduct of the study and manuscript preparation.
Attestation: Susumu Ueno approved the final manuscript.
Name: Nobuyuki Yanagihara, PhD.
Contribution: This author helped conduct of the study and manuscript preparation.
Attestation: Nobuyuki Yanagihara approved the final manuscript.
Name: Yuka Sudo, PhD.
Contribution: This author helped conduct of the study.
Attestation: Yuka Sudo approved the final manuscript.
Name: Yasuhito Uezono, MD, PhD.
Contribution: This author helped conduct of the study.
Attestation: Yasuhito Uezono approved the final manuscript.
Name: Takeyoshi Sata, MD, PhD.
Contribution: This author helped conduct of the study and manuscript preparation.
Attestation: Takeyoshi Sata approved the final manuscript.
This manuscript was handled by: Marcel E. Durieux, MD, PhD.

REFERENCES

1. Devane WA, Dysarz FA 3rd, Johnson MR, Melvin LS, Howlett AC. Determination and characterization of a cannabinoid receptor in rat brain. Mol Pharmacol 1988;34:605–13
2. Matsuda LA, Lolait SJ, Brownstein MJ, Young AC, Bonner TI. Structure of a cannabinoid receptor and functional expression of the cloned cDNA. Nature 1990;346:561–4
3. Munro S, Thomas KL, Abu-Shaar M. Molecular characterization of a peripheral receptor for cannabinoids. Nature 1993;365:61–5
4. Zias J, Stark H, Sellgman J, Levy R, Werker E, Breuer A, Mechoulam R. Early medical use of cannabis. Nature 1993;363:215
5. Pacher P, Bátkai S, Kunos G. The endocannabinoid system as an emerging target of pharmacotherapy. Pharmacol Rev 2006;58:389–462
6. Devane WA, Hanus L, Breuer A, Pertwee RG, Stevenson LA, Griffin G, Gibson D, Mandelbaum A, Etinger A, Mechoulam R. Isolation and structure of a brain constituent that binds to the cannabinoid receptor. Science 1992;258:1946–9
7. Pertwee RG, Ross RA. Cannabinoid receptors and their ligands. Prostaglandins Leukot Essent Fatty Acids 2002;66:101–21
8. Costa B, Vailati S, Colleoni M. SR 141716A, a cannabinoid receptor antagonist, reverses the behavioural effects of anandamide-treated rats. Behav Pharmacol 1999;10:327–31
9. Mason DJ Jr, Lowe J, Welch SP. Cannabinoid modulation of dynorphin A: correlation to cannabinoid-induced antinociception. Eur J Pharmacol 1999;378:237–48
10. Welch SP, Huffman JW, Lowe J. Differential blockade of the antinociceptive effects of centrally administered cannabinoids by SR141716A. J Pharmacol Exp Ther 1998;286:1301–8
11. Calignano A, La Rana G, Giuffrida A, Piomelli D. Control of pain initiation by endogenous cannabinoids. Nature 1998;394:277–81
12. Richardson JD, Kilo S, Hargreaves KM. Cannabinoids reduce hyperalgesia and inflammation via interaction with peripheral CB1 receptors. Pain 1998;75:111–9
13. Guindon J, De Léan A, Beaulieu P. Local interactions between anandamide, an endocannabinoid, and ibuprofen, a nonsteroidal anti-inflammatory drug, in acute and inflammatory pain. Pain 2006;121:85–93
14. Sagar DR, Kendall DA, Chapman V. Inhibition of fatty acid amide hydrolase produces PPAR-alpha-mediated analgesia in a rat model of inflammatory pain. Br J Pharmacol 2008;155:1297–306
15. Karbarz MJ, Luo L, Chang L, Tham CS, Palmer JA, Wilson SJ, Wennerholm ML, Brown SM, Scott BP, Apodaca RL, Keith JM, Wu J, Breitenbucher JG, Chaplan SR, Webb M. Biochemical and biological properties of 4-(3-phenyl-[1,2,4] thiadiazol-5-yl)-piperazine-1-carboxylic acid phenylamide, a mechanism-based inhibitor of fatty acid amide hydrolase. Anesth Analg 2009;108:316–29
16. Tsou K, Brown S, Sañudo-Peña MC, Mackie K, Walker JM. Immunohistochemical distribution of cannabinoid CB1 receptors in the rat central nervous system. Neuroscience 1998;83:393–411
17. Farquhar-Smith WP, Egertová M, Bradbury EJ, McMahon SB, Rice AS, Elphick MR. Cannabinoid CB(1) receptor expression in rat spinal cord. Mol Cell Neurosci 2000;15:510–21
18. Hohmann AG, Herkenham M. Localization of central cannabinoid CB1 receptor messenger RNA in neuronal subpopulations of rat dorsal root ganglia: a double-label in situ hybridization study. Neuroscience 1999;90:923–31
19. Chemin J, Monteil A, Perez-Reyes E, Nargeot J, Lory P. Direct inhibition of T-type calcium channels by the endogenous cannabinoid anandamide. EMBO J 2001;20:7033–40
20. Mackie K, Lai Y, Westenbroek R, Mitchell R. Cannabinoids activate an inwardly rectifying potassium conductance and inhibit Q-type calcium currents in AtT20 cells transfected with rat brain cannabinoid receptor. J Neurosci 1995;15:6552–61
21. Maingret F, Patel AJ, Lazdunski M, Honoré E. The endocannabinoid anandamide is a direct and selective blocker of the background K(+) channel TASK-1. EMBO J 2001;20:47–54
22. Fan P. Cannabinoid agonists inhibit the activation of 5-HT3 receptors in rat nodose ganglion neurons. J Neurophysiol 1995;73:907–10
23. Poling JS, Rogawski MA, Salem N Jr, Vicini S. Anandamide, an endogenous cannabinoid, inhibits Shaker-related voltage-gated K+ channels. Neuropharmacology 1996;35:983–91
24. Mendiguren A, Pineda J. Cannabinoids enhance N-methyl-D-aspartate-induced excitation of locus coeruleus neurons by CB1 receptors in rat brain slices. Neurosci Lett 2004;363:1–5
25. Catterall WA. From ionic currents to molecular mechanisms: the structure and function of voltage-gated sodium channels. Neuron 2000;26:13–25
26. Catterall WA, Goldin AL, Waxman SG. International Union of Pharmacology. XLVII. Nomenclature and structure-function relationships of voltage-gated sodium channels. Pharmacol Rev 2005;57:397–409
27. Wood JN, Boorman JP, Okuse K, Baker MD. Voltage-gated sodium channels and pain pathways. J Neurobiol 2004;61:55–71
28. Cummins TR, Sheets PL, Waxman SG. The roles of sodium channels in nociception: implications for mechanisms of pain. Pain 2007;131:243–57
29. Decosterd I, Ji RR, Abdi S, Tate S, Woolf CJ. The pattern of expression of the voltage-gated sodium channels Na(v)1.8 and Na(v)1.9 does not change in uninjured primary sensory neurons in experimental neuropathic pain models. Pain 2002;96:269–77
30. Wang W, Gu J, Li YQ, Tao YX. Are voltage-gated sodium channels on the dorsal root ganglion involved in the development of neuropathic pain? Mol Pain 2011;7:16
31. Nicholson RA, Liao C, Zheng J, David LS, Coyne L, Errington AC, Singh G, Lees G. Sodium channel inhibition by anandamide and synthetic cannabimimetics in brain. Brain Res 2003;978:194–204
32. Kim HI, Kim TH, Shin YK, Lee CS, Park M, Song JH. Anandamide suppression of Na+ currents in rat dorsal root ganglion neurons. Brain Res 2005;1062:39–47
33. Horishita T, Eger EI 2nd, Harris RA. The effects of volatile aromatic anesthetics on voltage-gated Na+ channels expressed in Xenopus oocytes. Anesth Analg 2008;107:1579–86
34. Wiley JL, Dewey MA, Jefferson RG, Winckler RL, Bridgen DT, Willoughby KA, Martin BR. Influence of phenylmethylsulfonyl fluoride on anandamide brain levels and pharmacological effects. Life Sci 2000;67:1573–83

35. Wang GK, Russell C, Wang SY. State-dependent block of voltage-gated Na+ channels by amitriptyline via the local anesthetic receptor and its implication for neuropathic pain. Pain 2004;110:166–74
36. Ragsdale DS, McPhee JC, Scheuer T, Catterall WA. Molecular determinants of state-dependent block of Na+ channels by local anesthetics. Science 1994;265:1724–8
37. Osawa Y, Oda A, Iida H, Tanahashi S, Dohi S. The effects of class Ic antiarrhythmics on tetrodotoxin-resistant Na+ currents in rat sensory neurons. Anesth Analg 2004;99:464–71, table of contents
38. Poyraz D, Bräu ME, Wotka F, Puhlmann B, Scholz AM, Hempelmann G, Kox WJ, Spies CD. Lidocaine and octanol have different modes of action at tetrodotoxin-resistant Na(+) channels of peripheral nerves. Anesth Analg 2003;97:1317–24
39. Ouyang W, Herold KF, Hemmings HC Jr. Comparative effects of halogenated inhaled anesthetics on voltage-gated Na+ channel function. Anesthesiology 2009;110:582–90
40. Starowicz K, Malek N, Przewlocka B. Cannabinoid receptors and pain. Wiley Interdiscip Rev Membr Transp Signal 2013;2:121–32
41. Adams IB, Compton DR, Martin BR. Assessment of anandamide interaction with the cannabinoid brain receptor: SR 141716A antagonism studies in mice and autoradiographic analysis of receptor binding in rat brain. J Pharmacol Exp Ther 1998;284:1209–17
42. Wiley JL, Razdan RK, Martin BR. Evaluation of the role of the arachidonic acid cascade in anandamide's *in vivo* effects in mice. Life Sci 2006;80:24–35
43. Romero TR, Resende LC, Guzzo LS, Duarte ID. CB1 and CB2 cannabinoid receptor agonists induce peripheral antinociception by activation of the endogenous noradrenergic system. Anesth Analg 2013;116:463–72
44. Waxman SG, Dib-Hajj S. Erythermalgia: molecular basis for an inherited pain syndrome. Trends Mol Med 2005;11:555–62
45. Fertleman CR, Ferrie CD, Aicardi J, Bednarek NA, Eeg-Olofsson O, Elmslie FV, Griesemer DA, Goutières F, Kirkpatrick M, Malmros IN, Pollitzer M, Rossiter M, Roulet-Perez E, Schubert R, Smith VV, Testard H, Wong V, Stephenson JB. Paroxysmal extreme pain disorder (previously familial rectal pain syndrome). Neurology 2007;69:586–95
46. Theile JW, Cummins TR. Inhibition of Navβ4 peptide-mediated resurgent sodium currents in Nav1.7 channels by carbamazepine, riluzole, and anandamide. Mol Pharmacol 2011;80:724–34
47. Renganathan M, Cummins TR, Waxman SG. Contribution of Na(v)1.8 sodium channels to action potential electrogenesis in DRG neurons. J Neurophysiol 2001;86:629–40
48. Joshi SK, Mikusa JP, Hernandez G, Baker S, Shieh CC, Neelands T, Zhang XF, Niforatos W, Kage K, Han P, Krafte D, Faltynek C, Sullivan JP, Jarvis MF, Honore P. Involvement of the TTX-resistant sodium channel Nav 1.8 in inflammatory and neuropathic, but not post-operative, pain states. Pain 2006;123:75–82
49. Black JA, Nikolajsen L, Kroner K, Jensen TS, Waxman SG. Multiple sodium channel isoforms and mitogen-activated protein kinases are present in painful human neuromas. Ann Neurol 2008;64:644–53
50. Henry MA, Freking AR, Johnson LR, Levinson SR. Sodium channel Nav1.6 accumulates at the site of infraorbital nerve injury. BMC Neurosci 2007;8:56
51. Black JA, Liu S, Tanaka M, Cummins TR, Waxman SG. Changes in the expression of tetrodotoxin-sensitive sodium channels within dorsal root ganglia neurons in inflammatory pain. Pain 2004;108:237–47
52. Strickland IT, Martindale JC, Woodhams PL, Reeve AJ, Chessell IP, McQueen DS. Changes in the expression of NaV1.7, NaV1.8 and NaV1.9 in a distinct population of dorsal root ganglia innervating the rat knee joint in a model of chronic inflammatory joint pain. Eur J Pain 2008;12:564–72
53. Berta T, Poirot O, Pertin M, Ji RR, Kellenberger S, Decosterd I. Transcriptional and functional profiles of voltage-gated Na(+) channels in injured and non-injured DRG neurons in the SNI model of neuropathic pain. Mol Cell Neurosci 2008;37:196–208
54. Okuse K, Chaplan SR, McMahon SB, Luo ZD, Calcutt NA, Scott BP, Akopian AN, Wood JN. Regulation of expression of the sensory neuron-specific sodium channel SNS in inflammatory and neuropathic pain. Mol Cell Neurosci 1997;10:196–207
55. Coggeshall RE, Tate S, Carlton SM. Differential expression of tetrodotoxin-resistant sodium channels Nav1.8 and Nav1.9 in normal and inflamed rats. Neurosci Lett 2004;355:45–8
56. Cummins TR, Waxman SG. Downregulation of tetrodotoxin-resistant sodium currents and upregulation of a rapidly repriming tetrodotoxin-sensitive sodium current in small spinal sensory neurons after nerve injury. J Neurosci 1997;17:3503–14

OPEN ACCESS Freely available online

PLOS | ONE

Palliation of Bone Cancer Pain by Antagonists of Platelet-Activating Factor Receptors

Katsuya Morita[1,2,4☯], Seiji Shiraishi[2☯], Naoyo Motoyama[2,3☯], Tomoya Kitayama[4], Takashi Kanematsu[4], Yasuhito Uezono[2], Toshihiro Dohi[5]*

1 Department of Pharmacology, Faculty of Nursing, Hiroshima Bunka Gakuen University, Hiroshima, Japan, **2** Cancer Pathophysiology, Division National Cancer Center Research Institute, Tokyo, Japan, **3** Department of Dental Science for Health Promotion, Division of Integrated Health Sciences, Institute of Biomedical and Health Sciences, Hiroshima University, Hiroshima, Japan, **4** Department of Cell and Molecular Pharmacology, Division of Basic Life Science, Institute of Biomedical and Health Sciences, Hiroshima University, Hiroshima, Japan, **5** Department of Pharmacotherapy, Pharmaceutical Sciences, Nihon Pharmaceutical University, Saitama, Japan

Abstract

Bone cancer pain is the most severe among cancer pain and is often resistant to current analgesics. Thus, the development of novel analgesics effective at treating bone cancer pain are desired. Platelet-activating factor (PAF) receptor antagonists were recently demonstrated to have effective pain relieving effects on neuropathic pain in several animal models. The present study examined the pain relieving effect of PAF receptor antagonists on bone cancer pain using the femur bone cancer (FBC) model in mice. Animals were injected with osteolytic NCTC2472 cells into the tibia, and subsequently the effects of PAF receptor antagonists on pain behaviors were evaluated. Chemical structurally different type of antagonists, TCV-309, BN 50739 and WEB 2086 ameliorated the allodynia and improved pain behaviors such as guarding behavior and limb-use abnormalities in FBC model mice. The pain relieving effects of these antagonists were achieved with low doses and were long lasting. Blockade of spinal PAF receptors by intrathecal injection of TCV-309 and WEB 2086 or knockdown of the expression of spinal PAF receptor protein by intrathecal transfer of PAF receptor siRNA also produced a pain relieving effect. The amount of an inducible PAF synthesis enzyme, lysophosphatidylcholine acyltransferase 2 (LPCAT2) protein significantly increased in the spinal cord after transplantation of NCTC 2472 tumor cells into mouse tibia. The combination of morphine with PAF receptor antagonists develops marked enhancement of the analgesic effect against bone cancer pain without affecting morphine-induced constipation. Repeated administration of TCV-309 suppressed the appearance of pain behaviors and prolonged survival of FBC mice. The present results suggest that PAF receptor antagonists in combination with, or without, opioids may represent a new strategy for the treatment of persistent bone cancer pain and improve the quality of life of patients.

Citation: Morita K, Shiraishi S, Motoyama N, Kitayama T, Kanematsu T, et al. (2014) Palliation of Bone Cancer Pain by Antagonists of Platelet-Activating Factor Receptors. PLoS ONE 9(3): e91746. doi:10.1371/journal.pone.0091746

Editor: Theodore John Price, University of Arizona, United States of America

Received October 16, 2013; **Accepted** February 14, 2014; **Published** March 17, 2014

Funding: This work was supported in part by Grants-in Aid for Scientific Research (B) 22390349, (C) 21592421 and (C) 24592798 from the Japanese Society for Promotion of Sciences and by the National Cancer Center Research and Development Fund (23-A-30). The funders had no role in study design, data collection and analysis, decision to publish, or preparation of the manuscript.

Competing Interests: The authors have declared that no competing interests exist.

* E-mail: t-dohi@nichiyaku.ac.jp

☯ These authors contributed equally to this work.

Introduction

Pain in cancer is produced by pressure on, or chemical stimulation of, specialized pain-signalling nerve endings called nociceptors (nociceptive pain) or it may be caused by damage or illness affecting nerve fibers themselves (neuropathic pain) which is responsive to stimuli that are normally non-painful; allodynia. Bone cancer pain is one of the most common and usually serious pain conditions in cancer patients [1].

Opioids remain the mainstay of cancer pain management, but in addition to the acute side effects the long-term consequences of tolerance, dependency, hyperalgesia and the suppression of the hypothalamic/pituitary axis should be acknowledged. Because the current available treatments are relatively ineffective against bone cancer pain, almost half of cancer patients have inadequate pain control [2,3]. Thus, the development of novel analgesics effective at treating bone cancer pain are required.

We have previously suggested that platelet-activating factor (PAF) may be a mediator of neuropathic pain. PAF injection into the mouse spinal cord caused thermal hyperalgesia and tactile allodynia, which were at least in part mediated by spinal dysfunction of glycine receptor α3 (GlyRα3) and were blocked by PAF receptor antagonists [4,5]. Subsequent studies showed PAF receptor blockade reduced pain behaviors elicited in nerve injury models. A PAF receptor antagonist, CV-3988, injected near the dorsal root ganglion (DRG) in rats or mice lacking PAF receptors showed a reduction in tactile allodynia following spinal nerve injury [6]. Intrathecal injection of the PAF receptor antagonist, WEB 2086, a benzodiazepine derivative for 9 days post-surgery in rats suppressed the development of mechanical allodynia in a rat spared nerve injury model [7]. PAF receptor antagonists, TCV-309 (PAF related), BN 50739 (natural product related compound), and WEB 2086, produced profound and long lasting anti-allodynia effects in several different neuropathic pain

models in mice, including a partial sciatic nerve ligation injury model, a partial infraorbital nerve ligation model, a chronic constriction of the infraorbital nerve injury model (CCI model) and a streptozotocin (STZ)-induced diabetes model [8]. The evidence suggests that PAF contributes to neural tissue damage and pain behavior after nerve injury.

The animal models above investigated pain due to bone cancer, in which tumor cells are injected locally into the bone. The present study used the femur bone cancer (FBC) model in mice [9]. Animals were injected with osteolytic NCTC2472 cells, and subsequently the effects of PAF receptor antagonists on pain behaviors were evaluated.

Materials and Methods

Experimental Animals

The experiments were performed using male C3H/HeN mice (CLEA Japan, Inc., Tokyo), weighing 20–25 g. All experimental procedures and animal handling were performed according to both the Guiding Principles for the Care and Use of Laboratory Animals approved by the Japanese Pharmacological Society and the guidelines of Hiroshima University, Hiroshima, Japan and the guidelines of National Cancer Center Research Institute, Tokyo, Japan. The protocol was approved by the committee on the Ethics of Animal Experiments of the Hiroshima University (Permit Number: A-09-17 and A-11-16), and of the National Cancer Center (Permit Number: T11-004-M02). All surgery was performed under sodium pentobarbital anesthesia, and all efforts were made to minimize suffering. The animals were used for only one measurement in each experiment.

The Mouse Femur Bone Cancer (FBC) Model

For the FBC model, NCTC 2472 tumor cells (American Type Culture Collection, ATCC; Manassas, VA, USA) were injected into the medullary cavity of the distal femur of C3H/HeN mice [9]. The NCTC 2472 cells were maintained in Dulbecco's Modified Eagle's Medium, supplemented with 10% Fetal bovine serum, 100 unit/ml penicillin, and 100 μg/ml streptomycin (all products from Gibco Laboratories); and cultured at 37°C in a humidified atmosphere of 5% CO_2 then passaged weekly according to ATCC guidelines. For administration, cells were detached by scraping and then centrifuged at 900 rpm for 3 min. The pellet was suspended in Hank's balanced salt solution (HBSS) and then used for intratibial injection.

For implantation, tumor cells were injected following the protocol described previously by Honore et al. [9] with slight modification. In brief, C3H/HeN mice were anesthetized with a sodium pentobarbital (60 mg/kg) i.p. injected. For intratibial inoculation of cells, the right knee of each mouse was bent and placed facing the experimenter and a minimal skin incision was made exposing the tibial plateau. A 25 gauge dental reamer was used to perforate the tibial plateau and, once removed, a 30 gauge needle coupled to a Hamilton syringe filled with the cell suspension was carefully introduced into the medullary cavity of the tibia. Then, 10^5 NCTC 2472 cells suspended in 5 μl of HBSS were slowly injected (living cells). Control groups were injected with 5 μl of HBSS or HBSS containing 10^5 NCTC 2472 cells killed by quickly freezing and thawing them twice without cryoprotection and then washing with fresh HBSS (deaden cells). Finally, Caviton EX, a dental-grade hydraulic temporary sealant (GC Dental Products, Co. Ltd., Tokyo, Japan) was applied to the tibial plateau incised area and the surgical procedure was completed with stitching of the knee skin. Body weights were recorded for each mouse every 3 days throughout the study. The animals were euthanized following weight loss greater than 20% of body weight or upon demonstrating related symptoms such as serious ataxic movements or other neurological abnormalities due to ethical concerns.

Drug Administration

Gabapentin (1-(aminomethyl)-cyclohexaneacetic acid) was obtained from Sigma-Aldrich (St. Louis, MO). Morphine was obtained from Takeda Pharmaceutical Co., (Osaka, Japan). WEB 2086 (3-[4-(2-chlorophenyl)-9- methyl-6*H*-thieno[3,2-*f*][1,2,4]triazolo-[4,3-*a*][1,4]-diazepin-2-yl]-1-(4-morpholinyl)-1-propanone) was obtained from Tocris Bioscience (Ellisville, MO). TCV-309 (3-bromo-5-[*N*-phenyl-*N*-[2-[[2-(1,2,3,4-tetrahydro-2-isoquinolyl- carbonyloxy)ethyl]carbamoyl]ethyl]carbamoyl]-1-propylpyridinium nitrate), and BN 50739 (tetrahydro-4,7,8,10methyl-(chloro-2phenyl)6[dimethoxy-3,4- phenylthio]-methylthiocarbonyl-9 pyrido[4′,3′-4,5]thieno[3,2-*f*]triazolo-1,2,4[4,3-*a*]diazepine-1,4) were donated from Takeda Pharmaceutical Co., and Institute Henri Beaufour, respectively.

TCV-309 and WEB 2086 were each dissolved in sterile artificial cerebrospinal fluid (ACSF) or saline solution. BN 50739 was dissolved in a solvent containing 25% 2-hydroxypropyl-β-cyclodextrin (Sigma/RBI, Natick, MA) and distilled water, pH adjusted to ~6 using 1 N NaOH, and diluted appropriately with ACSF or saline. Other reagents were dissolved in ACSF or saline. The drug solutions were freshly prepared on each experimental day. ACSF composition (in mM) was NaCl 142, KCl 5, $CaCl_2$ $2H_2O$ 2, $MgCl_2 \cdot 6H_2O$ 2, NaH_2PO_4 1.25, D-glucose 10, HEPES 10, pH 7.4. TCV-309, BN70329, or WEB 2086 was administered intravenously 30 min-3 hr before pain assessment.

Knockdown of PAF Receptor in the Spinal Cord

Knockdown of PAF receptor was performed according to a previous report [5]. siRNAs were incorporated into the hemagglutinating virus of the Japan (HVJ)-Envelope Vector according to the manufacturer's instructions. Briefly, after mixing 40 μl (1 assay unit, AU) of HVJ-Envelope Vector with 4 μl of the enclosing factor, the mixture was centrifuged (10,000×*g*, 10 min, 4°C), and the pellet suspended in 10 μl of buffer solution. Then, 10 μl of a mixture of 3 siRNAs solution (#1, #2 and #3, 1 μg/μl each) was added, and the mixture was kept on ice for 5 min. Sterile ACSF (10 μl) containing synthetic siRNA duplexes (0.45 pmole/animal) was injected into the subarachnoid space between the L5 and L6 vertebrates of conscious mice. The sequences of the siRNA oligonucleotide (sense) were as follows: PAF receptor (#1, 5′-CACCUCAGUGAGAAGUUUUACAGCA-AG-3′; #2, 5′-ACCCUUCCAAGAAACUAAAUGAGAU-AG-3′; #3, 5′-CAACUUCCAUCAGGCUAUUAAUGAU-AG-3′; targeting sequences around position 1005 to 1029, 232 to 256, 893 to 917, respectively, in *paf*r, GenBank accession no. D5087). Moreover, mismatched siRNA with three or four nucleotide mismatches was prepared to examine nonspecific effects of siRNA duplexes (siRNA#4, 5′-ACUCUGCCAAGAGACUACAUGAGAU-AG-3). These selected sequences were also submitted to a BLAST search (Bioinformatics Center Institute for Chemical Research, Kyoto University, Japan) against the mouse genome sequence to ensure that only one gene in the mouse genome was targeted. siRNAs were purchased from iGENE Therapeutics Inc. (Tsukuba, Japan).

Behavioral Analysis in the FBC Model

The behavioral analysis was preformed following the protocol described previously [5,10]. The pain-related behaviors in the FBC model were evaluated before and after drug administration on 11 days after tumor implantation. The experimental and sham

operated animals were evaluated for on-going pain based on guarding behavior, for ambulatory pain based on limb-use abnormality, and for allodynia-like behavior based on the von Frey filament test and paintbrush test. Guarding behavior, limb-use abnormality and allodynia-like pain were assessed in the same animals. The mice were placed in a clear plastic observation box and allowed to habituate for 15 min. Then, spontaneous guarding behavior was assessed during a 2-min observation period. The lifting time of the hind paw on the ipsilateral side during ambulation was measured as guarding behavior. Limb-use abnormality was scored on a scale of 0 to 4: 0, normal use of limb; 1, slight limp; 2, clear limp; 3, partial non-use of limb; and 4, complete non-use of limb. Allodynia-like behavior was assessed by lightly stroking the injured leg with a paintbrush (allodynia score) or evaluated by measuring the paw withdrawal threshold in response to probing with a series of calibrated fine filaments (allodynia threshold) as reported previously [5]. The allodynia score was ranked as described by Minami et al. [11]: 0, no response; 1, mild squeaking with attempts to move away from the stroking probe; 2, vigorous squeaking, biting the stroking probe and strong efforts to escape from the stroking probe. Values are the average of the total score evaluated 3 times at each time point (possible maximum score at each time point: 2/mouse). The guard times were significantly prolonged at 5 and 6 days after tumor implantation compared with the values at pre-implantation. Similarly, animals also started to exhibit abnormal limb-use at 5 days after tumor implantation, and such abnormal behavior was more prominent in the later days. The allodynia threshold was evaluated by measuring the paw withdrawal threshold in response to probing with von Frey monofilaments, and significant threshold declines were observed after the 3rd day post tumor implantation compared with the values at pre-implantation, and the decrease reached a peak after 5 and 7 days. The allodynia score was evaluated by measuring the ranked response to lightly stroking with a paintbrush, and significant score rises were observed after the 4-day post tumor implantation compared with the values at pre-implantation, and the increase reached a peak after 6 and 8 days. Throughout the experiment, behavioral testing was performed under blind conditions by a single experimenter. Injections were performed blind by another person. Intrathecal injection was performed as described previously [4].

Determination of Lyso-PAF-Acetyltransferase (Lyso-PAF AT)/Lysophospha- tidylcholine Acyltransferase 2 (LPCAT2), a PAF Synthesis Enzyme

The lumbar regions of the spinal cord (L2-L6) were obtained from sham-operated (deaden cells implanted) or tumor-bearing mice. The spinal cord tissues (4.8–5.0 mg) were homogenized in 20 mM Tris-HCl (pH 7.5) containing 1 mM EDTA, 1 mM EGTA, 10 mM NaF, 10 mM β-glycerophosphate and 1 μg/ml of various protease inhibitors (benzamdine, leupeptin and anti-pain). The homogenate was reacted with 0.6% NP-40 for 5 min at 4°C, followed by centrifugation at 15,000 rpm for 5 min at 4°C and the supernatant was obtained. The supernatant was mixed at a volume ration of 4:1 in 10 mM Tris-HCl (pH 6.8) containing 10% (v/v) glycerol, 2% sodium dodecylsulfate (SDS), 0.01% bromophenol blue and 0.5% β-mercaptoethanol, with subsequent boiling at 70°C for 30 min.

Immunoblotting Assays

The obtained samples were electrophoresed for 2 hr at room temperature on polyacrylamide gels (stacking gel 3% and separating gel 10%) and then blotted to polyvinylidene fluoride membranes previously treated with 100% methanol. The transferred proteins on the membranes were blocked by incubating with blocking solution, a 5% skim milk-containing wash buffer (20 mM Tris-HCl (pH 7.5), 137 mM NaCl and 0.1% Tween 20), at 25°C for 1 hr. The membranes were exposed to the primary antibody as follows: against LPCAT2 (1:1,000; Sigm); against β-actin (1:1,000; IM-GENEX Innovations in Functional Genomics, SanDiego, CA) diluted with the wash buffer containing 1% skim milk overnight at 4°C, followed by washing three times with the wash buffer, and then incubation with a secondary antibody as follows: for the LPCAT2 antibody and β-actin antibody, an anti-rabbit IgG antibody conjugated with horseradish peroxidase (1:2,000; DakoCytomation, Glostrup, Denmark) at room temperature for 1 hr. The membranes were again rinsed three times with the wash buffer and developed with an enhanced chemiluminescence (ECL) western detection system (ECL reagents, purchased from Thermo Fisher Scientific, and Nacalai Tesque Inc., Kyoto Japan; ImageQuant^{TM} LAS 4000 mini detection system, GE healthcare Japan, Tokyo, Japan). The density of each band was analyzed using NIH Image software, and the densitometric units were corrected using the value of β-actin. The data are expressed as the mean ± SEM.

Morphine-induced Constipation

Mice were provided food and water ad libitum before the test period, and both (with or without TCV-309) groups consumed comparable amounts of food prior to the test as measured over a 24-hr period in the test environment. No food or water was available during the test. Mice were caged in acrylic boxes with grid floors suspended over filter paper. Fecal boli were collected from each group of mice every hour for 1 hr following the injection of saline or various doses of morphine and the weight of fecal boli was recorded as an index of the constipating effects of morphine.

Generation of Kaplan–Meier Survival Curves

The health of the mice was examined daily. Mice that presented with signs of ill health were killed by cervical dislocation according to the recommendations of our Ethical Committee. In our experience, these signs precede the time of death by a couple of days. The time of death was recorded for each mouse that was found dead or was killed. Kaplan–Meier survival curves were generated using Graphpad Prism software (version 4; Graphpad, Inc, San Diego, CA).

Statistical Analyses

All data are reported as values of the mean ± SEM (standard error of the mean). Graphpad Prism software version 4 was used to perform the statistical analysis. Regarding the statistical analysis of the pain-related behaviors, comparisons of the allodynis score, withdrawal threshold, guarding behavior and limb-use abnormality of the differences between the drug-treated groups and the vehicle-treated group were evaluated using two-way ANOVA followed by Tukey-Kramer test, or an unpaired Student's *t*-test. Comparisons of median survival were performed using log-rank and Gehan–Breslow–Wilcoxon tests. A probability value (P) of <0.05 was considered statistically significant.

Results

Effects of Systemic Administration of Specific PAF Receptor Antagonists on Tactile Allodynia and Pain Behaviors in FBC Model Mice

Effects of TCV-309 on allodynia and pain behaviors (guarding behavior and limb-use abnormality) were examined in FBC model

mice. TCV-309 with a range of 10–300 μg/kg by i.v. dose-dependently reduced the allodynia score (Figure 1A) and increased the withdrawal threshold (Figure 1B) at 11 to 15 days after tumor implantation in the mice. The effects of TCV-309 were quite long lasting. For instance, TCV-309 significantly ameliorated mechanical allodynia by a single injection of 100 μg/kg, i.v. with a peak effect at 1 to 2 days after the injection up to 6 days. Guarding behavior was continuously aggravated during the observation period, while limb-use abnormality reached a maximal response and continued during the period (Figure 1C, 1D). Guarding behavior and limb-use abnormality were also improved by TCV-309. TCV-309 up to 1 mg/kg did not affect general behavior or motor function estimated by the RotaRod test (data not shown). Other PAF receptor antagonists, BN 50739 and WEB 2086, also ameliorated the allodynia and pain behaviors in the FBC model mice (Figure1E–1H).

Effects of Blockade of Spinal PAF Receptors on Allodynia and Pain Behaviors in FBC Model Mice

To confirm the site of cancer pain palliation by PAF antagonists, the effects of intrathecal injection of TCV-309 and WEB 2086, and also interference in the expression of spinal PAF receptors using siRNA of PAF receptor mRNA were examined. Spinal administration of 10 pg of these drugs 13 days post-tumor implantation produced rapid and marked suppression of tactile allodynia with the maximal effect at 1 day post-implantation and significantly suppressed the allodynia within 4 days (Figure 2A). Pain release effects evaluated by withdrawal threshold, guarding behavior and limb-use abnormality of intrathecal injection of TCV-309 and WEB 2086 were also achieved (Figure 2B–2D).

Knockdown of the expression of spinal PAF receptor protein was achieved by intrathecal transfer of PAF receptor siRNA in mice. As previously reported, a significant reduction in PAF receptor expression in normal mice and mice 15 days after surgery on the sciatic nerve, reaching 37.5±5.4% and 29.9±4.9% of the control at 3 days after siRNA transfection, respectively, while the expression was not altered by the HVJ-E vector alone or mismatched siRNA [5]. By siRNA transfection 13 days post-tumor implantation, the allodynia score, withdrawal threshold, guarding behavior an limb-use abnormality were improved with the peak effect at 2 to 3 days after siRNA transfection, while the pain-relief action gradually disappeared over 9 days (Figure 3E–3H). Injection of mismatched siRNA had no effect on the development of allodynia and pain behaviors. The amount of LPCAT2 protein significantly increased in the spinal cord at 8, 15 and 30 days after transplantation of NCTC 2472 tumor cells into mice tibia (Figure 3). The results support the concept that PAF increase in the spinal cord of tumor-bearing mice may relate to pain production and that the site of pain-relief action of the PAF receptor antagonists involve the spinal cord in FBC mice.

Potentiation of the Analgesic Effect by Combination of PAF Receptor Antagonists with Morphine

Bone cancer pain is one of the most severe types of cancer pain and is often resistant to treatment even with opioid analgesics. Combinations of opioids and non-opioid analgesics are usual practice to obtain a better analgesic effect in clinical practice. Combined administration of morphine with TCV-309 was examined (Figure 4A). Morphine 0.1 and 0.3 mg/kg injection 1 day after TCV-309 3 and 10 μg/kg administration produced a marked reduction in the allodynia score at 30 min after morphine

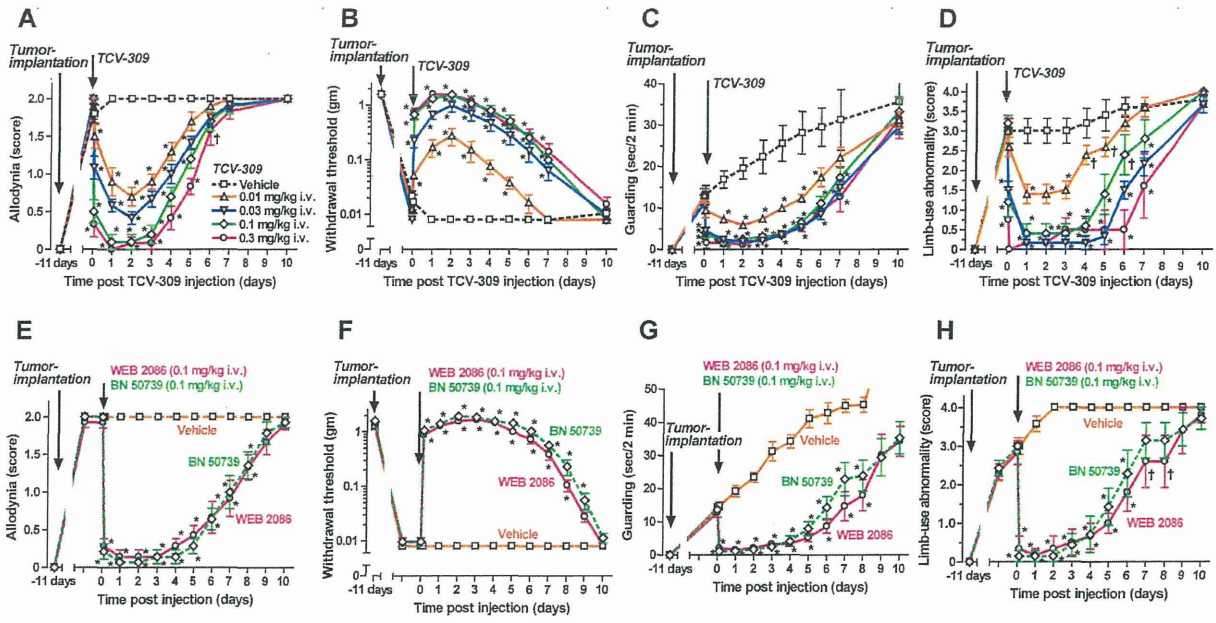

Figure 1. Effects of PAF-receptor antagonists on tactile allodynia (A, B, E, F), guarding behavior (C, G) and limb-use abnormality (D, H) in the femur bone cancer (FBC) mice. TCV-309 0.01-0.3 mg/kg, WEB 2086 0.1 mg/kg, BN 50739 0.1 mg/kg or a vehicle were intravenously injected at 11 days post tumor transplantation. Control mice received injections with a vehicle: saline or 25% 2-hydroxypropyl-β-cyclodextrin. The pain-related behaviors that developed after tumor implantation in mice were not affected by vehicle treatments. Values represent the mean ± SEM. n = 11 mice per group. †P<0.05, *P<0.01 compared with the corresponding control (vehicle treated) values, as determined by analysis of variance followed by Tukey-Kramer test.
doi:10.1371/journal.pone.0091746.g001

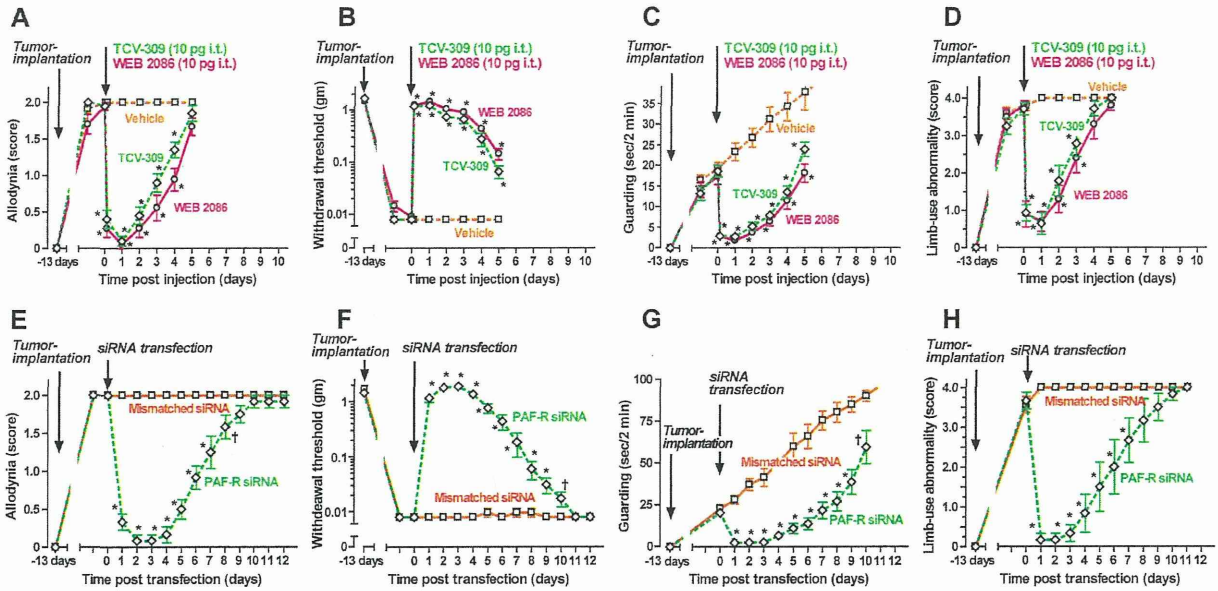

Figure 2. Effects of blockade of PAF receptors by intrathecal injection of PAF receptor antagonists (A–D) or knockdown of spinal PAF receptors by siRNA (E–H) on tactile allodynia (A, B, E, F), guarding behavior (C, G) and limb-use abnormality (D, H) in FBC mice. (A–D); Tumor cells were implanted into the intramedulla of left femur bone 13 days before the intrathecal (i.t.) injection of PAF receptor antagonists. TCV-309 (10 pg/mouse), WEB 2086 (10 pg/mouse) or the vehicle were injected intrathecally at time "0". Data are expressed as the mean ± SEM., n = 8–12 mice per group. *P<0.01 compared with the corresponding control (vehicle treated) values, as determined by analysis of variance followed by Tukey-Kramer test. Control mice received injections with a vehicle: ACSF. The pain-related behaviors that developed after tumor implantation in mice were not affected by the vehicle treatments. (E–H); siRNA or mismatched siRNA of PAF-receptor mRNA were transfected into the spinal cord 13 days after tumor implantation. Data are expressed as the mean ± SEM. n = 8–10 mice per group. †P<0.05, *P<0.01 compared with the corresponding control (mismatched siRNA transfection) values, as determined by analysis of valiance followed by an unpaired Student's *t*-test. Control mice received injections with mismatched siRNA or a vehicle: HVJ-envelope only. The pain-related behaviors that developed after tumor implantation in mice were not affected by mismatched siRNA or vehicle treatments.
doi:10.1371/journal.pone.0091746.g002

injection and the effect returned to each level of TCV-309 alone at 3 to 4 hrs after the administration. The combination of morphine 1 mg/kg with gabapentin 10 mg/kg i.v. had no significant anti-allodynia effect (Figure 4B). A large dose of gabapentin, 30 mg/kg, was required to produce a transient anti-allodynia effect. Morphine alone had little analgesic effect at 0.3 to 3 mg/kg, s.c. and a small effect at 10 mg/kg in the FBC model. A higher dose of 30 mg/kg of morphine was less effective (Figure 4C).

The dose-response relation of TCV-309 and morphine in combination is shown in Figure 4D and Figure 4E. Morphine 0.3 mg/kg and TCV-309 0.1–1.0 μg/kg at each dose alone had no anti-allodynia effect, but in combination, the allodynia score decreased by more than 90% depending on the dose of TCV-309 (Figure 4D). Morphine in combination with TCV-309 10 μg/kg as low as 0.03 mg/kg produced a significant anti-allodynia effect and abolished the allodynia response at 0.3 mg/kg (Figure 4E). Eight days after the injection of TCV-309, WEB 2086 and BN 50739, pain relieving effect of these compounds became not significant (Figure 5). However, the additional administration of morphine 0.3 mg/kg still markedly ameliorated allodynia and pain behaviors (Figure 5). These results showed that PAF receptor antagonists achieves long-lasting potentiation of the analgesic effect when morphine was administered.

Effect of PAF Receptor Antagonists on Morphine-induced Constipation

Constipation is one of the most common side-effects of morphine and it appears in almost all patients treated with morphine. If the obstacle effect of morphine on intestinal activity is not potentiated, this side effect of morphine could be reduced by reducing the dosage of morphine without disturbing the analgesic effect. Morphine reduced the amount of feces from 1 mg/kg s.c. and abolished it more than 10 mg/kg. The dose-dependent constipation effect of morphine was not affected by TCV-309 10 μg/kg (Figure 6).

Repeated Administration of TCV-309 Protected Against the Appearance of Pain-like Behavior

As the anti-allodynia effect of TCV-309 was long-lasting, the effect of the repeated administration was examined. In control mice, tactile allodynia appeared at 3 days after tumor implantation and reached to peak response at 8 days. Guarding behavior appeared at 10 days post tumor implantation and gradually increased over 30 days, while limb-use abnormality appeared at 8 days and reached a maximum at about 16 days post implantation (Figure 7A–7D). Injection of TCV-309 at 0.3 mg/kg, i.v. was started on the day mice were implanted with the tumor and was continued every 4 days for 28 days. Pain behaviors evaluated by allodynia score, withdrawal threshold, guarding behavior and limb-use abnormality did not appear during dosing (Figure 2). Thus, the treatment with TCV-309 before pain arose protected against crisis of pain and tolerance to TCV-309 analgesia did not develop.